

# Aqueous Angiography in Normal Canine Eyes

Jessica B. Burn<sup>1</sup>, Alex S. Huang<sup>2</sup>, Arthur J. Weber<sup>1</sup>, Andras M. Komáromy<sup>1</sup>,  
and Chris G. Pirie<sup>1</sup>

<sup>1</sup> Michigan State University Veterinary Medical Center, East Lansing, MI, USA

<sup>2</sup> Doheny Eye Institute, University of California, Los Angeles, Los Angeles, CA, USA

**Correspondence:** Chris G. Pirie,  
Michigan State University Veterinary  
Medical Center, 736 Wilson Road,  
East Lansing, MI 48824, USA. e-mail:  
[piriechr@msu.edu](mailto:piriechr@msu.edu)

**Received:** July 29, 2019

**Accepted:** August 2, 2020

**Published:** August 28, 2020

**Keywords:** canine; aqueous humor;  
aqueous angiography; fluorescein;  
indocyanine green; conventional  
outflow

**Citation:** Burn JB, Huang AS, Weber  
AJ, Komáromy AM, Pirie CG. Aqueous  
angiography in normal canine eyes.  
*Trans Vis Sci Tech.* 2020;9(9):44,  
<https://doi.org/10.1167/tvst.9.9.44>

**Purpose:** To conduct aqueous angiography (AA) using a clinically applicable technique in normal dogs and to compare findings to intravenous scleral angiography (SA).

**Methods:** We examined 10 canine cadaver eyes and 12 eyes from live normal dogs. A gravity-fed trocar system delivered 2% sodium fluorescein and 0.25% indocyanine green (ICG) intracamerally (IC) in cadaver eyes. In vivo AA was subsequently performed in one eye of each of the 12 dogs via IC bolus of ICG under sedation. The same 12 dogs received SA via intravenous ICG (mean  $\pm$  SD) 10.7  $\pm$  3.3 days later. Identical scleral sectors were imaged using a Spectralis confocal scanning laser ophthalmoscope.

**Results:** The gravity-fed trocar system permitted visualization of the conventional aqueous humor outflow (CAHO) pathways in cadaver eyes, but not in vivo. Fluorescence was observed superonasally in four of the 10 cadaver eyes within 24.0  $\pm$  3.6 seconds. A single IC bolus of ICG showed CAHO pathways in vivo, demonstrating sectoral outflow patterns in the superotemporal sclera in 10 of the 12 eyes within 35.0  $\pm$  4.3 seconds; four of the 12 eyes exhibited pulsatile aqueous movement. SA exhibited fluorescence patterns comparable to AA with weak pulsatile aqueous humor outflow.

**Conclusions:** Angiography (AA or SA) in dogs permits visualization of the CAHO pathway and its vascular components in vivo. AA may be a more useful modality to assess aqueous humor outflow.

**Translational Relevance:** Intracameral AA has potential utility for evaluating CAHO in vivo in dogs, an important animal model species.

## Introduction

Aqueous humor outflow has been well documented in numerous species, including dogs, cats, rabbits, and non-human primates.<sup>1–5</sup> Aqueous humor exits the eye via two separate routes: the conventional route and the unconventional route. The conventional aqueous humor outflow (CAHO) pathway involves egress of aqueous humor via the trabecular meshwork into Schlemm's canal or the venous plexus, whereas the unconventional pathway involves uveoscleral, uveovortex, and uveolymphatic absorption of aqueous humor through the uvea and passage into the choroidal circulation.<sup>6,7</sup> Although anatomical similarities exist between dog and human eyes, it is important to note that dogs, in contrast to humans, have an angular aqueous plexus and not a true Schlemm's canal.<sup>8,9</sup>

The CAHO pathway plays a major role in maintaining a physiologic intraocular pressure (IOP) and accounts for approximately 85% of the total aqueous humor outflow in dogs, whereas unconventional aqueous humor outflow encompasses about 15%.<sup>10</sup> Passage of aqueous humor through the trabecular meshwork and into the systemic circulation via the CAHO pathway is driven by a pressure gradient moving from inside the eye toward the distal outflow vessels.<sup>11</sup> In contrast, aqueous humor outflow through the unconventional pathway is passively regulated by osmotic gradients and is not reliant on IOP.<sup>12</sup> Alterations to outflow facility in either the conventional or unconventional routes are believed to play a major role in glaucoma. To date, little is known regarding the in vivo characteristics of canine aqueous humor outflow.

Investigation of the post-trabecular distal aqueous humor outflow tract as a source of increased

resistance is gaining momentum within the physician-based literature.<sup>13,14</sup> Although little has been published on this topic in dogs, several studies have identified the vascular and microvascular structures associated with the CAHO pathways of dogs via corrosion casting techniques.<sup>1,2</sup> Casting dyes injected via an intracameral (IC) route readily moved from the anterior chamber into the intrascleral venous plexus of Hovius.<sup>1</sup> The CAHO pathways have been shown to be comprised of complex networks. One study noted redundancy of CAHO pathways with anastomosis among the aqueous collector channels and the intrascleral venous plexus of Hovius in some dogs, but in others very little branching or deviation was observed.<sup>1</sup> These casting techniques highlight the complexity of the CAHO pathways but fail to provide insight into their true role and clinical application in regulating IOP in vivo.

Numerous angiographic techniques following the intravenous (IV) and IC delivery of a dye have been conducted in animals and humans, permitting direct visualization of aqueous outflow or the ocular vasculature.<sup>5,15–20</sup> Aqueous angiography (AA) aims to provide information regarding the aqueous humor outflow and drainage pathways present within the eye by administering a fluorescent dye directly into the anterior chamber.

At the present time, there are no published data regarding AA in live dogs. Most prior works have focused on utilizing ex vivo models<sup>20–22</sup>; however, recent studies conducted in living human patients have demonstrated the diagnostic potential of this imaging technique.<sup>15,16</sup> A similar approach was performed ex vivo with dogs and cats<sup>23,24</sup> and in vivo in cats,<sup>25</sup> rabbits,<sup>26</sup> and non-human primates<sup>5</sup> to provide baseline descriptions in normal animals. Aqueous angiography is believed to have a strong clinical application in the future management of glaucoma due to mechanical obstructions of aqueous humor outflow. This study aims to outline a clinical approach for conducting in vivo AA, which will directly assess the CAHO pathways in live dogs. Similar to AA, intravenous scleral angiography (SA) has been successfully performed in humans.<sup>16</sup> Scleral angiography highlights the flow of a fluorescent dye through the scleral plexus, with certain points overlapping with aqueous humor outflow channels.<sup>27,28</sup> Episcleral veins have been identified based on their depth and location within the scleral tissue,<sup>16</sup> and laminar flow patterns have been used to help indicate flow characteristics of blood within the scleral vessels.<sup>29,30</sup> Thus, a secondary objective of this study was to explore the potential utility of SA in live dogs.

## Materials and Methods

### General Experimental Outline

To evaluate AA and to refine its clinical technique for use in the dog, a series of experimental studies were conducted (Table 1). One day prior to conducting angiography in live dogs, all animals received a complete physical and ophthalmic examination, which included a Schirmer tear test I (Merck Animal Health, Madison, NJ), topical fluorescein staining (Ful-Glo; Akorn, Decatur, IL), slit-lamp biomicroscopy (Kowa SL-17; Kowa Company, Tokyo, Japan), rebound tonometry (TONOVET; Icare USA, Raleigh, NC), and indirect ophthalmoscopy (Keeler All Pupil II; Keeler Instruments, Broomall, PA). Imaging of either the left or right eye was selected based on their normality, with efforts made to achieve an equal distribution between left and right eyes. In cases where the same dog was imaged more than once, the same eye was imaged for comparative purposes with a recovery period of at least 7 days. Data collected included history, breed, gender, age, and relevant ophthalmic diagnostics (e.g., IOP, tear test values). Complete ophthalmic examinations were also performed immediately following the completion of angiography and daily thereafter for up to 1 week to monitor for any potential post-procedure changes or complications. All studies were carried out in compliance with the ARVO Statement for the Use of Animals in Ophthalmic and Vision Research and were approved by the Michigan State University Institutional Animal Care and Use Committee.

### Experiment 1: Ex Vivo Aqueous Angiography in Canine Cadaver Eyes

The experimental setup for conducting AA in 10 canine cadaver eyes was designed based on recent published works performed in human subjects and is shown in Figure 1.<sup>5,15,23,24</sup> Eyes were from dogs euthanized for reasons unrelated to this study. Owner consent was obtained for all dogs. The experimental setup was modified to include direct manometry to ensure that IOP was consistently maintained at 20 mm Hg<sup>23</sup> (McLellan GJ, et al. *IOVS*. 2019;60:ARVO Abstract 3184). The setup was comprised of two separate systems: a gravity-fed fluid delivery trocar system and a pressure monitoring trocar system.

The 10 cadaver globes utilized for AA were placed in an anatomically correct orientation, ensuring that the optic nerve was directed inferonasally to match that of a dog in sternal recumbency. A 23-gauge trocar system (Disposable One Step Cannula System; Dorc, Exeter,

**Table 1.** Experimental Group Summary

Experiment	Route of Administration	ICG Dose	ICG Concentration	In Vivo or Ex Vivo
1, 2	Gravity-fed trocar system	Constant gravity-fed flow	Exact concentration unknown	Ex vivo (Experiment 1) and in vivo (Experiment 2), imaged within 1 hour of euthanasia
3	Single IC injection	0.1 mL	0.25%	In vivo
4	Single IV injection	1 mg/kg	0.25%	In vivo

Shown for Experiments 1 through 4 are the routes of administration, doses, and concentrations of ICG employed in addition to those performed ex vivo or in vivo.

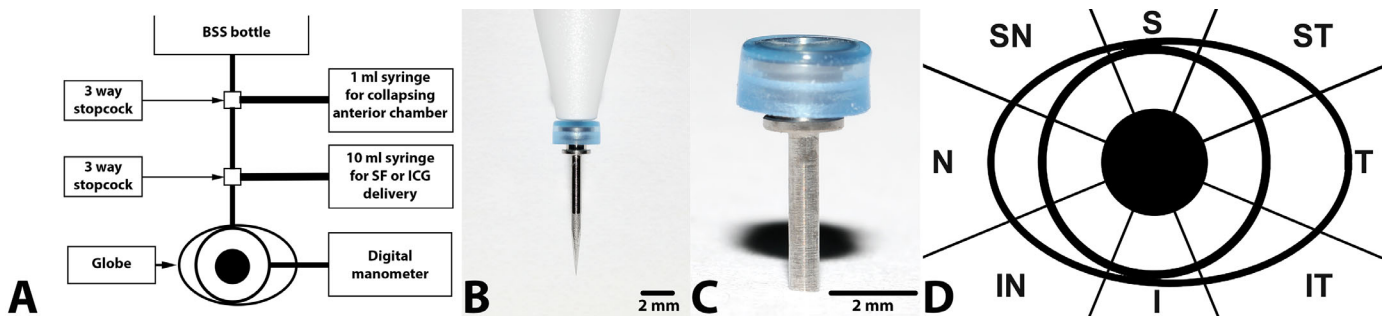


**Figure 1.** (A) Schematic representation of the gravity-fed fluid delivery and pressure monitoring systems. (B) Photographs of the trocar delivery system, insertion cannula, and trocar. (C) Close-up of valved trocar employed for conducting AA in the ex vivo (cadaver) experimental setup. (D) Schematic representation of scleral division into sectors. BSS and adjustment of the bottle height were employed to maintain IOP as determined via a digital manometer. The 1-mL syringe was utilized to collapse the anterior chamber, and the 10-mL syringe contained 2% sodium fluorescein or 0.25% ICG, permitting entry into the anterior chamber. The globe was sectioned into octants to allow for consistent documentation of location. S, superior; T, temporal; I, inferior; N, nasal; ST, superotemporal; IT, inferotemporal; IN, inferonasal; SN, superonasal.

NH), attached to a balanced salt solution (BSS) fluid reservoir, was inserted through the superior limbus into the anterior chamber to maintain a normal physiologic IOP value (20 mm Hg).<sup>31</sup> The eye was perfused with BSS for a total of 1 hour (Fig. 1).<sup>20–22,32</sup> A second 23-gauge trocar system connected to a digital manometer (Traceable Products, Webster, TX) was inserted through the inferior limbus of the globe, permitting direct IOP measurements. The manometer was calibrated by the manufacturer, and consistency was shown between this device and rebound tonometry (TONOVET). The TONOVET was calibrated by the manufacturer within less than 1 year before and after the study.

The height of the BSS reservoir was adjusted until the IOP was stabilized at 20 mm Hg prior to introduction of the angiographic dye into the anterior chamber. As the delivery system was gravity fed, no quantification of dye volume or concentration entering the anterior chamber was performed. For conducting sodium fluorescein AA, 2% sodium fluorescein

(AK-Fluor 10%; Akorn, Decatur, IL) was used. For indocyanine green (ICG) AA, 0.25% ICG (Diagnostic Green, Farmington Hills, MI) was administered. Imaging of all limbal scleral sectors was performed using an en face view, including the superior, inferior, nasal, and temporal aspects and all possible scleral regions in between (Fig. 1D). These sectors were observed for visualization of fluorescent dye using a Spectralis confocal scanning laser ophthalmoscope (Heidelberg Engineering, Heidelberg, Germany) as described below. Different sectors were imaged based on where fluorescence was observed.

## Experiments 2, 3, and 4: In Vivo Aqueous Angiography in Canine Eyes

### General Study Protocol and Pre-Medication

All live dogs received a single subcutaneous injection of a non-steroidal anti-inflammatory medication, carprofen, at 4.4 mg/kg (Rimadyl; Zoetis, Parsippany, NJ) 1 hour prior to performing angiography.

All dogs received maropitant citrate, 1.0 mg/kg subcutaneous (SQ) (Cerenia; Zoetis) and diphenhydramine hydrochloride, 2.0 mg/kg SQ (Bioniche Pharma, Lake Forest, IL) 20 minutes prior to injection of the dye; these medications were used as a prophylactic measure to counteract potential emesis and anaphylaxis, respectively, associated with dye administration.<sup>33</sup> Blood pressure was not recorded for Experiments 3 and 4 due to the use of heavy sedation. A pulse oximeter was used to monitor vital statistics (heart rate, oxygen saturation level) in sedated dogs.

### Experiment 2: In Vivo Aqueous Angiography Using a Gravity-Fed Trocar System

A pilot study was performed on four purpose-bred dogs to evaluate the feasibility of conducting AA in vivo using the gravity fed trocar system. All dogs underwent general anesthesia and were continuously monitored during the procedure. Pre-procedure and post-procedure IOPs were measured using rebound tonometry.

### Experiment 3: In Vivo Aqueous Angiography Via Single Intracameral Injection

Twelve normal, purpose-bred dogs were heavily sedated, and AA was performed through IC dye administration. Four of these dogs underwent AA utilizing trocars 2 weeks prior. A sterile 20-gauge IV catheter was placed in either the right or left cephalic vein. All dogs received a standard sedation protocol consisting of butorphanol 0.3 mg/kg IV and dexmedetomidine 6 µg/kg IV (Dexdomitor; Zoetis).

The right eye was selected for the first six dogs and the left for the remaining six dogs; however, in the case of the four dogs that recently underwent AA, the same eye was imaged for comparative purposes. When a dog had been adequately sedated, the ocular surface was anesthetized by administering topical proparacaine hydrochloride 0.5% ophthalmic solution. The periocular skin and ocular surface were aseptically prepped with dilute 2% povidone-iodine solution. Two stay sutures (4-0 silk) were placed to allow for centration of the globe.<sup>5</sup> Rebound tonometry was used prior to and after injection of ICG. The eyelids were manually retracted to provide adequate exposure of the globe, with particular attention to minimizing any external pressure onto the globe itself. Aqueous angiography was subsequently performed via IC injection of 0.1 mL of 0.25% ICG under steady pressure using a 25-gauge needle and 1-mL syringe. The needle was

placed within the superonasal limbal sector and tunneled to achieve a tight seal and help minimize extrusion of ICG and subconjunctival bleb formation. Imaging of all visible scleral sectors was performed as described below. After imaging was complete, sedation in all dogs was reversed with atipamezole intramuscularly (IM) (Antisedan; Zoetis) at a dose equivalent to the volume of dexmedetomidine administered. Upon recovery, the IOP of all dogs was measured, and the dogs were treated with neomycin-polymyxin B-dexamethasone ophthalmic ointment every 12 hours for 2 days to address the potential for mild intraocular inflammation or infection resulting from aqueous paracentesis or suture placement.

### Experiment 4: In Vivo Intravenous Scleral Angiography

The same eye of each of the 12 dogs that underwent in vivo AA by a single IC injection was subsequently imaged using 0.25% ICG IV using the same sedation protocol as Experiment 3. Imaging was performed following a recovery period of  $10.7 \pm 3.3$  days. Rebound tonometry was performed before and after administration of the ICG dye. For conducting SA, a total of 1 mg/kg ICG was injected IV under steady pressure via the catheterized cephalic vein. Imaging was performed as described below. Reversal, post-procedural monitoring, and treatment were similar to that employed for Experiment 3.

### Aqueous Angiography Imaging and Optical Coherence Tomography

All angiographic imaging was performed using a Heidelberg Spectralis confocal scanning laser ophthalmoscope fitted with a 55° lens. Automatic real-time tracking was employed to maximize still-image quality. The imaging sequence for AA was initiated upon entrance of angiographic dye into the anterior chamber, using the appropriate settings (i.e., 488-nm excitation laser and 500-nm barrier filter for sodium fluorescein and 790-nm excitation laser and 830-nm barrier filter for ICG). Imaging was performed every 5 seconds for a total duration of 20 minutes; this timeline allowed at least 5 minutes of imaging without any further changes seen in dye movement. Video recordings with a frame rate of 30 frames per second were obtained and were time stamped to permit accurate temporal documentation. En face views allowed for the entire sclera to be imaged in the cadaver eyes. Because of the nictitating membrane covering the superonasal, nasal, and infer-



onasal aspects of the globe, only the superior, superotemporal, temporal, and inferotemporal sectors of the sclera were consistently imaged *in vivo*.

When the dogs had been adequately sedated and positioned, and immediately prior to SA, standard color images (Canon EOS 5D Mark IV with Canon EF 100mm f/2.8L Macro IS USM lens; Canon, Tokyo, Japan) were obtained of each visible scleral sector for comparative purposes. For IV SA, the imaging sequence was initiated immediately following the rapid bolus of dye administration, and the superior, superotemporal, temporal, and inferotemporal scleral sectors were imaged for each eye. Video footage was recorded for 40 seconds post-bolus, followed by a combination of still images and video sequences thereafter for a total time period of 10 minutes after dye administration; this approach allowed at least 5 minutes of imaging without any further observable changes in dye movement. Optical coherence tomography (OCT) using the Heidelberg Spectralis and an anterior segment lens provided cross-sectional information of the sclera and observation of luminal vessels in sectors where fluorescence was observed.

### Measurements and Data Analysis

Angiograms were reviewed by two separate individuals independently (JB, CP) upon completion of each study. A subjective qualitative analysis was provided for each angiogram. Descriptive statistics were employed for each study group (means, standard deviations) for evaluating time at which angiographic dye was injected IC or IV (time zero) to time of visualization of dye within the CAHO pathways. Values recorded by each observer were averaged; however, no statistical analysis (e.g., interclass correlation) comparing graders was performed due to the small sample size. Absolute differences and individual standard deviations between individuals imaged were calculated based on each grader's recorded values. The number and location of outflow pathways and the presence or absence of circumferential vessels, bifurcations, or intricate collateral pathways were recorded. In eyes where visualization of the CAHO pathways was detected after IC and IV administration of ICG dye, cross-sectional scans using OCT were obtained to verify the presence of scleral vessels. Angiographic techniques (IC vs. IV) were compared through subjective characterization of the capacity of each route to provide clear visibility of the CAHO pathways. Additionally, digital overlays of identical scleral sectors, comparing angiographic techniques, were generated using Photoshop (Adobe, San Jose, CA) via the color render command. All eyes

pre- and post-experimentation were evaluated using the Standardization of Uveitis Nomenclature (SUN) scale.<sup>34</sup> Absolute differences, individual standard deviations, and relative changes in IOP were calculated to evaluate pre- and post-IOP results between Experiments 3 and 4 (Tables 3 and 4).

## Results

### Experiment 1: Ex Vivo Aqueous Angiography in Canine Cadaver Eyes

The 10 eyes used in this experiment were obtained from eight mixed breed dogs, one Chihuahua, and one Havanese (Table 2). The gravity-fed trocar system employed was found to be relatively easy to use and permitted adequate control and regulation of IOP to maintain a pressure of 20 mm Hg. Use of the valved trocar system allowed easy entry within the anterior chamber, and no detectable leakage surrounding the trocars was noted. Dye fluorescence within the CAHO pathways was visualized in a total of eight of the 10 dog eyes imaged (80%). Time to fluorescence within the CAHO pathways, regardless of the dye employed, was  $24 \pm 3.6$  seconds following entry into the anterior chamber. Noted outflow patterns were highly variable in their presentation, ranging from solitary vessels within a single quadrant exhibiting minimal branching patterns to extensive and complex vascular networks (Fig. 2). Sectoral variation was also noted amongst the eyes imaged (Fig. 3). No notable difference in the observed intensity of fluorescence was observed between locations. Diffusion of sodium fluorescein was observed over time, hindering visualization. No cross-sectional OCT scans were obtained.

### Experiment 2: In Vivo Aqueous Angiography Using a Gravity-Fed Trocar System

Four eyes from three intact female beagles and one intact male mixed-breed dog underwent *in vivo* AA using the gravity-fed trocar system (data not shown). Visualization of ICG fluorescence was absent in all visible scleral quadrants and the sectors in between those quadrants in the four eyes imaged. No cross-sectional OCT imaging was performed due to the lack of visibility of ICG fluorescence (data not shown). This approach was found to be impractical and cumbersome, with the disadvantage of not producing any visible dye movement into the CAHO pathways and vascular channels. This experiment was performed to validate the *ex vivo* method for *in vivo* use. To improve

**Table 2.** Summary of Dogs Utilized for Conducting Ex Vivo Aqueous Angiography

ID	Sex	Age (mo)	Breed	Eye	Onset of Fluorescence Post-Injection (s)	Vessel Location	IOP Throughout Imaging (mm Hg)
1	F	2	Mixed	OS	28	Not visualized	20
2	F	2	Mixed	OD	18	Superonasal	20
3	F	5	Mixed	OD	19	Nasal	20
4	F	5	Mixed	OS	22	Inferonasal	20
5	F	96	Chihuahua	OS	25	Superonasal	20
6	F	96	Chihuahua	OS	24	Superior	20
7	M	2	Mixed	OD	23	Superonasal	20
8	M	144	Havanese	OS	27	Superior, temporal, nasal	20
9	F	144	Havanese	OS	29	Superior, temporal, nasal, some inferior	20
10	M	2	Mixed	OS	25	Not visualized	20

M, male; F, female; OD, right eye; OS, left eye.

accessibility of the procedure, the gravity-fed trocar system was replaced with a single bolus injection protocol (Experiment 3).

### Experiment 3: In Vivo Aqueous Angiography Via Single Intracameral Injection

A total of 12 dogs were utilized for conducting AA following a single IC injection of dye (Table 3). Heavy sedation in conjunction with topical anesthesia provided adequate restraint and immobilization necessary for stay suture placement and conducting IC administration of ICG. There was no difference in imaging outcome from the four dogs that had undergone more procedures, as compared to the other eight dogs. Intraocular pressure was measured immediately prior to IC injection of ICG and within 15 minutes after injection of the dye. Individual pre- and post-IOP results, absolute differences, individual standard deviations, and relative change in IOP are listed in Table 3. An average of 25 still images were obtained for each eye using the Heidelberg Spectralis.

Following IC injection of ICG, diffuse fluorescence throughout the anterior chamber was readily observed. Shortly thereafter, dye fluorescence was observed emanating into various scleral sectors in 10 of the 12 eyes imaged. Two eyes failed to demonstrate fluorescence within any scleral sectors evaluated. Upon exiting the anterior chamber, initial dye fluorescence was noted to occur within intrascleral

channels, occurring on average  $35.0 \pm 4.3$  seconds after IC injection of ICG. Although no statistical analysis was performed, the means provided by the two graders were consistent. The mean absolute difference between the two graders was 0.4 seconds, and the mean individual standard deviation was 0.27 seconds. Progressive and rapid filling of larger, complex radially oriented luminal networks was noted shortly thereafter (Fig. 4). The most common scleral sector to exhibit dye fluorescence associated with the CAHO pathways was the superotemporal sclera. Results demonstrating regional fluorescence among the eyes imaged are summarized in Figure 5. Numerous bifurcations and intricate collateral pathways were present in nine eyes, with one eye exhibiting a single lateral vessel. In six of the 10 eyes that demonstrated intrascleral fluorescence, dye movement was noted to exhibit progressive and complete delineation of the vessel walls once observed (Fig. 6). Thereafter, observed fluorescence intensity remained uniform and static. In four of the 12 eyes (33.3%), pulsatile and turbulent movement of dye was observed, demonstrating a unidirectional movement in two of the eyes (16.7%), whereas the other two eyes exhibited bidirectional movement (16.7%) (Supplementary Movie S1). Noted pulsations were intermittent throughout the angiograms, when present, but appeared to coincide with the heart rate of the dog. All outflow channels that exhibited fluorescence following IC administration of ICG were readily identifiable on cross-sectional OCT as vessels.

**Table 3.** Summary of Dogs Utilized for Conducting In Vivo Aqueous Angiography

ID	Sex	Age (y)	Body Weight (kg)	Eye	Onset of Fluorescence Post-injection (s)	Vessel Location	Vessel Complexity and Pulsation	(A) Pre-Injection	(B) Post-Injection	IOP (mm Hg)		
										Absolute Difference (A-B)	Individual SD	Change (B-A)/A
1	F	3.87	10	OD	30	Superotemporal	Complex, bifurcations	16	8	8	5.66	-0.50
2	F	3.89	10	OD	45	Superotemporal	Complex, bifurcations	11	18	7	4.95	0.64
3	M	5.87	20.6	OD	35	Superotemporal-temporal	Single vessel	11	4	7	4.95	-0.64
4	F	3.90	9	OD	35	Superotemporal	Complex, bifurcations, bidirectional pulsation	11	9	2	1.41	-0.18
5	M	2.17	11	OD	35	Not visualized	None	12	5	7	4.95	-0.58
6	F	2.38	11.5	OS	35	Superotemporal and temporal	Complex, bifurcations, pulsation	22	5	17	12.02	-0.78
7	F	1.55	9	OS	30	Superotemporal	Complex, bifurcations	14	19	5	3.54	0.36
8	F	1.57	9	OS	35	Superotemporal	Complex, bifurcations	10	20	10	7.07	1.00
9	M	2.61	12.9	OS	30	Superotemporal, temporal, inferotemporal	Complex, bifurcations, bidirectional pulsation	14	20	6	4.24	0.43
10	F	2.61	11.5	OS	35	Faint superotemporal and temporal vessels	Complex, bifurcations	9	22	13	9.19	1.44
11	M	1.60	15.2	OS	40	Superotemporal, temporal, inferotemporal	Complex, bifurcations, pulsation	12	25	13	9.19	1.08
12	F	1.60	12	OD	35	Not visualized	None	21	9	12	8.48	-0.57
Mean		2.80	11.81		35.00			13.58	13.67	8.92	6.31	0.14
SD		1.33	3.32		4.26			4.17	7.66	4.19	—	0.78

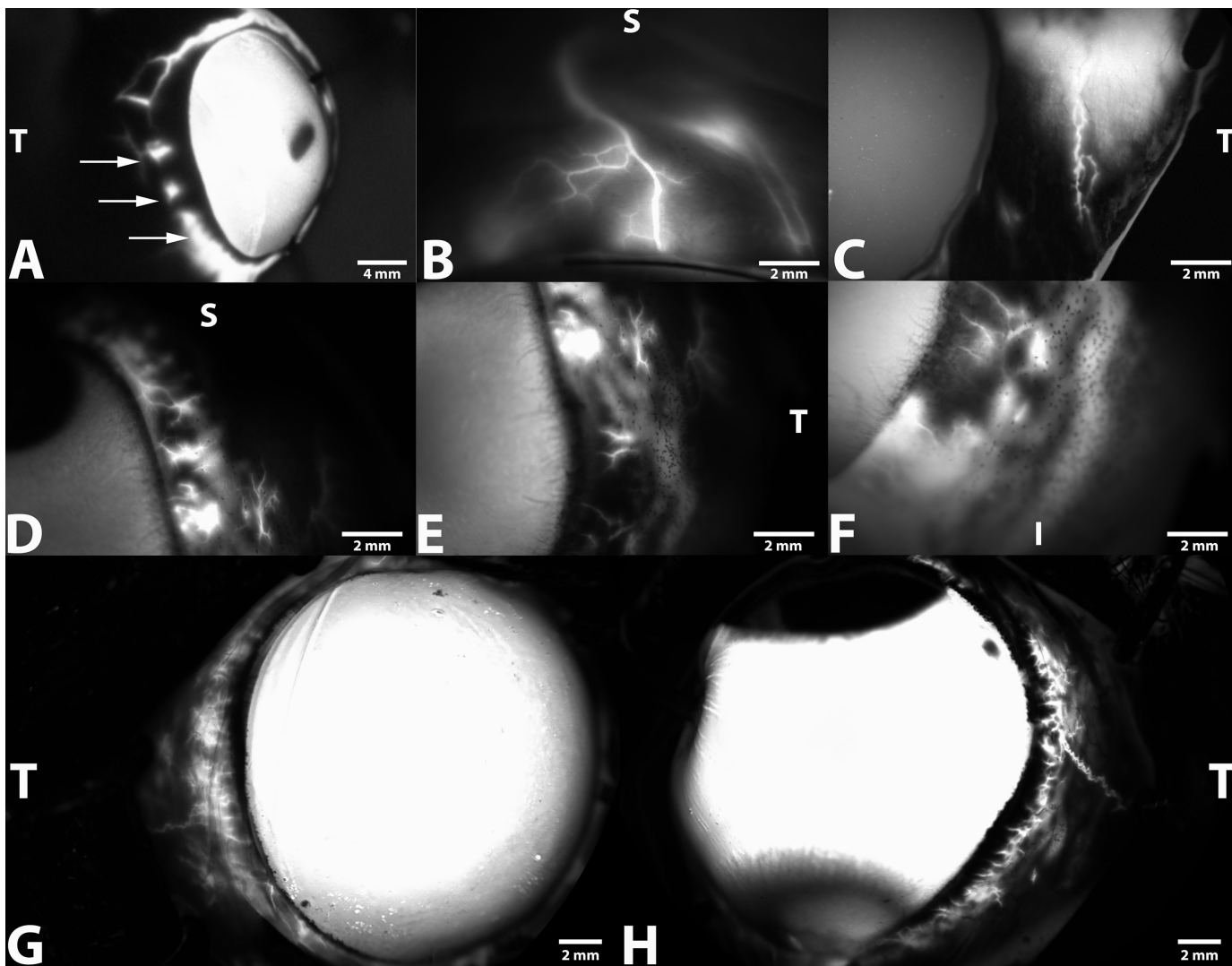


**Figure 2.** Representative AA images obtained from five dog cadaver eyes using a gravity-fed trocar system and sodium fluorescein. Images depict intraspecies and regional differences associated with the CAHO pathways observed. (A) The right globe from a 5-month-old spayed female mixed-breed dog depicts large circumferential vessels with minimal bifurcation within the superior, temporal, and inferior scleral sectors 10 minutes after dye entry into the anterior chamber. Note the marked extravasation of sodium fluorescein (arrows). (B) Fluorescence and visualization of a solitary CAHO pathway within the superior scleral sector (10 minutes) within the right globe from a 5-month-old spayed female mixed-breed dog. (C) Extensive circumferential vessels, demonstrating numerous complex and intricate collateral channels, can be seen (10 minutes) within the temporal scleral sector in the left eye from an 8-year-old mixed-breed dog. (D–F) Images depict regional differences associated with the CAHO pathways at 3 minutes following dye entry into the anterior chamber within the superior (D), temporal (E), and inferior (F) scleral sectors of the same eye from a 6-month-old mixed-breed dog. (G, H) Images of the right eye (G) and left eye (H) depict variations associated with the CAHO pathways between eyes noted at 5 minutes from the same 8-year-old mixed-breed dog. S, superior; T, temporal; I, inferior.

#### Experiment 4: In Vivo Intravenous Scleral Angiography

Following a 7-day recovery period, the same eyes of all 12 dogs that underwent AA via a single IC injection were evaluated using conventional IV administration of ICG and scleral imaging (Table 4). All eyes prior to imaging were considered clinically normal and did not exhibit any evidence of intraocular inflammation

or dye fluorescence (i.e., following prior ICG administration from Experiment 3). Intraocular pressure was measured immediately prior to IV injection of ICG and within 15 minutes after the injection of dye.

Filling patterns among the 12 eyes imaged were noted to be highly variable. Common trends were observed and characterized by the rapid and progressive filling of large circumferential intrascleral vessels, consistent with the venous circle of Hovius, 3 to 5 mm



**Table 4.** Summary of Dogs Utilized for Conducting In Vivo Scleral Angiography

ID	Eye	Onset of Fluorescence Post-Injection(s)	IOP (mm Hg)		Absolute Difference (A – B)	Individual SD $\sqrt{[(A - B)^2/2]}$	Change (B – A)/A
			(A) Pre-Injection	(B) Post-Injection			
1	OD	30	14	18	4	2.83	0.29
2	OD	45	9	7	2	1.41	-0.22
3	OD	35	13	8	5	3.54	-0.38
4	OD	35	10	7	3	2.12	-0.30
5	OS	30	15	11	4	2.83	-0.27
6	OS	35	16	9	7	4.95	-0.44
7	OD	35	19	12	7	4.95	-0.37
8	OS	35	23	20	3	2.12	-0.13
9	OS	30	7	4	3	2.12	-0.43
10	OS	35	16	13	3	2.12	-0.19
11	OS	40	14	12	2	1.41	-0.14
12	OD	30	17	11	6	4.24	-0.35
Mean		34.58	14.42	11.00	4.08	2.89	-0.24
SD		4.50	4.40	4.57	1.78	—	0.20

**EXPERIMENT 1 SEGMENTAL VARIATION**

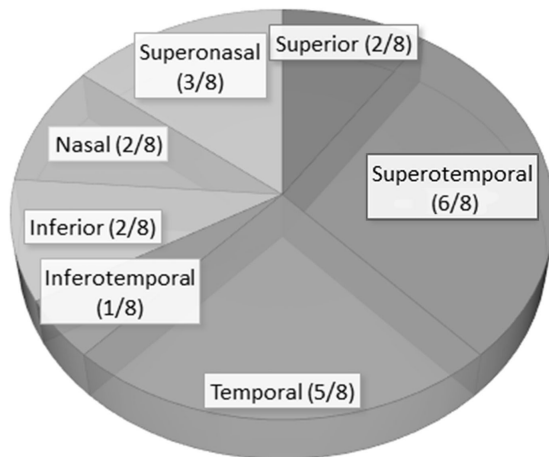


**Figure 3.** Schematic demonstrating the sectoral variation in visualization of fluorescent dye, based on scleral sectors, administered IC in 10 ex vivo canine eyes. Fluorescence and visualization of the CAHO pathways were seen in eight of the 10 eyes.

from the limbus (Fig. 7). Numerous anastomoses were observed between these large caliber vessels. Shortly thereafter, filling of smaller, deeper intrascleral vessels was observed. These vessels were thought to represent components of the intrascleral venous plexus. Simultaneously during this later filling period, fluorescence within both superficial and deep conjunctival arteries followed by their venular counter parts occurred. In

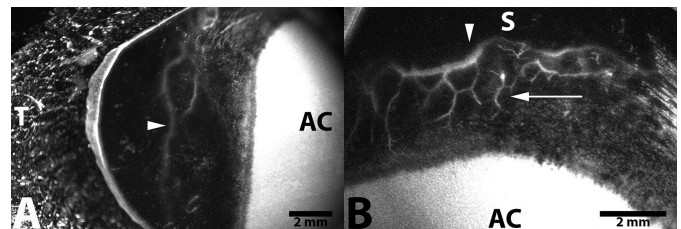


**Figure 4.** Representative in vivo AA image following IC injection of ICG into the right eye of a 3-year-old intact female beagle dog. Fluorescence with deep intrascleral vessels (arrow) and a large circumferential vessel (arrowhead) is readily visualized within the (A) temporal scleral quadrant (9 minutes after injection) and (B) superior scleral quadrant (15 minutes after injection). AC, anterior chamber; S, superior; T, temporal.

all but one eye imaged, visualization of fluorescence within the vasculature was progressive and uniform. In this 1 eye, visible pulsation and turbulent flow was observed within the deeper intrascleral vessels. Dye movement during this early filling period also demonstrated bidirectional movement (Supplementary Movie S2). All dogs recovered uneventfully following imaging.

**Comparison of Intracameral and Intravenous Routes of Injection**

When qualitatively comparing noted intrascleral vessels, IC ICG injection corresponded with IV routes of ICG administration in 10 of 12 eyes imaged (83.3%) (Figs. 8, 9). Two dogs could not be assessed due to a

### EXPERIMENT 3 SEGMENTAL VARIATION

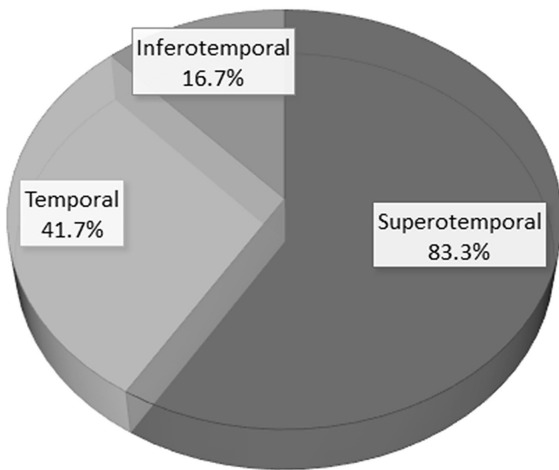


**Figure 5.** Schematic demonstrating the sectoral variation in fluorescent dye outflow after intracameral administration in 12 live dogs. The most frequent scleral sector to exhibit dye fluorescence associated with the CAHO pathways was the superotemporal scleral aspect (10 of 12 eyes, 83.3%). This location was the first to show fluorescence and exhibited the most intense dye fluorescence. Five eyes (41.7%) also demonstrated fluorescence of ICG within the temporal scleral quadrant, and two additional eyes (16.7%) also displayed fluorescence within the inferotemporal scleral sector.

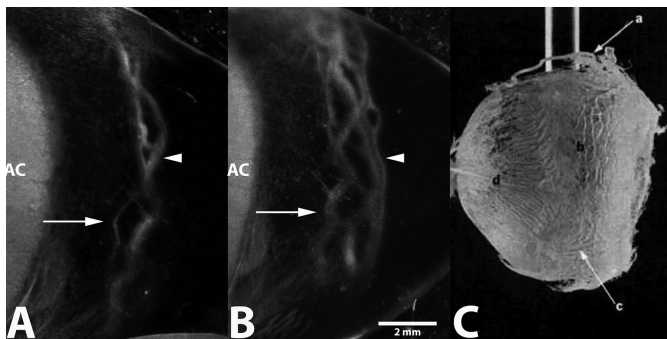


**Figure 6.** Representative in vivo AA image following IC injection of ICG into the left eye of a 1-year-old intact female beagle dog. Initial fluorescence at 1 minute (A) and progressive filling at 4 minutes (B) after injection is depicted within deep intrascleral vessels (*arrow*) and larger circumferential vessels (*arrowhead*). AC, anterior chamber. Corrosion cast image is from previous studies by van Buskirk et al.<sup>1</sup> to show similarities in the location and luminal diameter of intrascleral vessels and the circle of Hovius (labeled b). Image used with permission.

lack of visualization of dye fluorescence following IC administration. When visible, the IC route of administration allowed for visualization of the intrascleral venous plexus, in addition to regional components of the venous circle of Hovius. Additionally, using this modality, pulsatile motion of dye was readily observed. One of the dogs exhibited pulsatile movement of dye following IC administration and transient movement

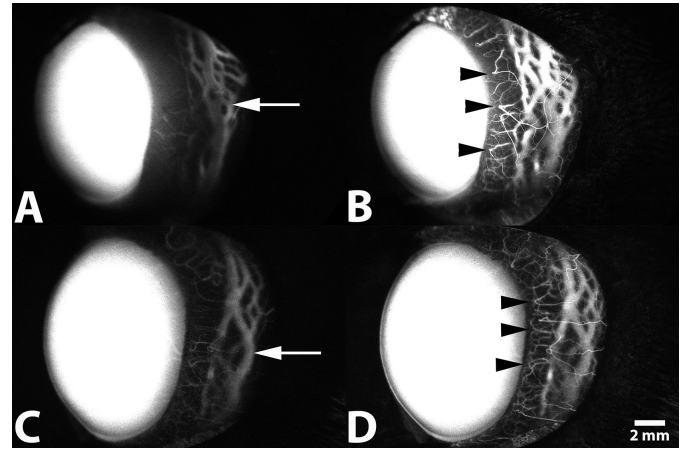


**Figure 7.** Representative SA following IV administration of ICG of the left eye from a 1-year-old intact female beagle dog (A, B) and from a 2-year-old male beagle dog (C, D). (A, C) Filling within deep circumferential ciliary arteries, the intrascleral venous plexus, and the venous circle of Hovius within the lateral scleral quadrant is visualized 30 seconds after injection (*arrow*). (B, D) Filling of terminal ciliary arterioles, capillary beds, and venular counterparts is visualized 1 minute after injection (*arrowhead*).

following IV administration. In contrast, IV administration of ICG accommodated rapid visualization of both the intrascleral venous plexus and venous circle of Hovius, in addition to the conjunctival and episcleral vasculature. However, no significant movement of dye, suggestive of aqueous humor outflow, was readily visible beyond the initial luminal filling of the vessels with this technique. In all eyes where fluorescence of ICG was noted following IC administration, similar vascular components were identifiable on side-by-side comparisons following an IV route of administration. Cross-sectional OCT scans qualitatively verified the congruency of luminal pathways seen in both the IC and IV routes of dye administration (Fig. 10). Direct overlay comparing routes of administration and color rendering, using a commercially available software, demonstrated slight variation among the fluorescent patterns observed (Fig. 8). Luminal fluorescence following IV administration demonstrated complete filling of the vascular channels observed. Partial and/or incomplete fluorescence, specifically along the luminal walls of the larger vascular channels associated with the venous circle of Hovius, was noted following IC administration.

### Safety

No aqueous flare (0 on the SUN scale) was observed in any eye prior to IC injections. All 12 dogs recovered from sedation and administration of ICG without significant complications. One day following the

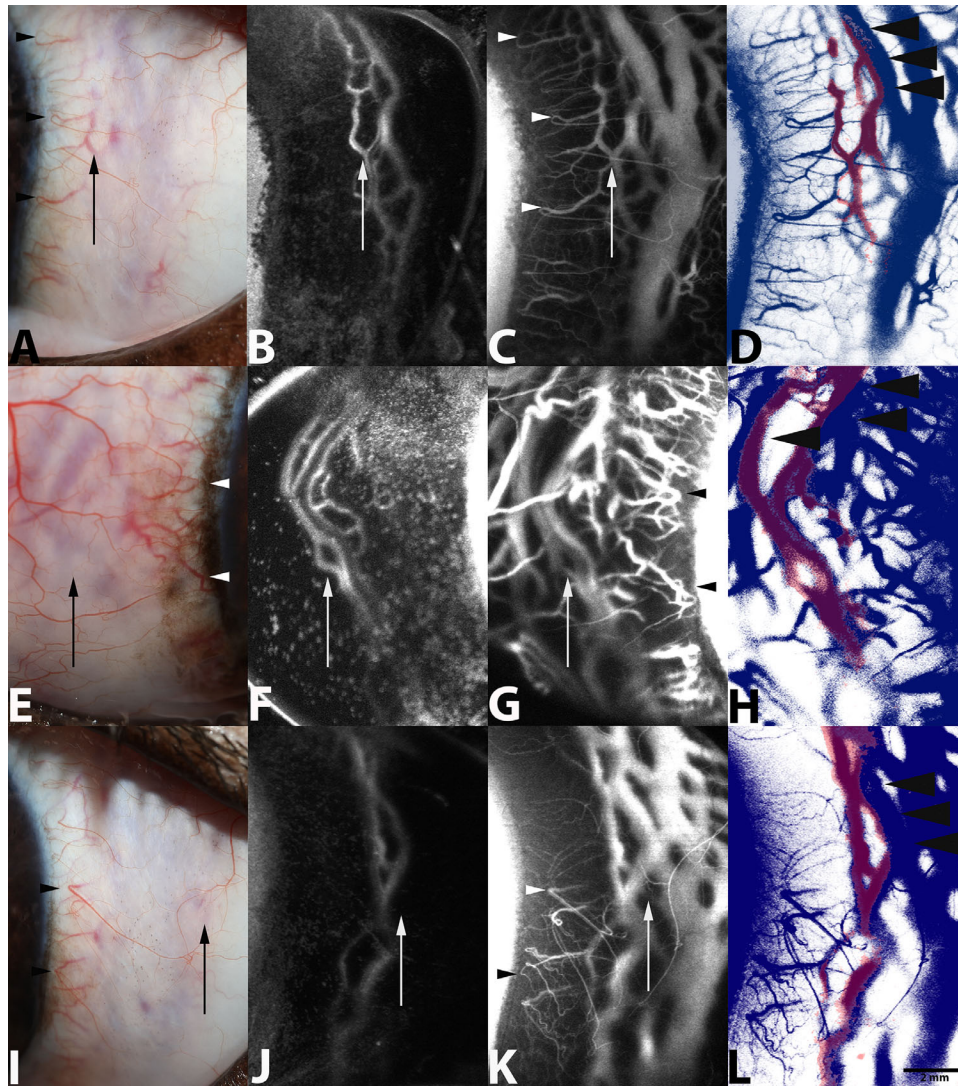


**Figure 8.** Representative standard color (A, E, I), *in vivo* IC AA (B, F, J), and IV SA (C, G, K) using ICG dye from the left eye of a 1-year-old intact female beagle dog (A–C), the right eye of a 3-year-old intact female beagle (E–G), and the left eye of a 1-year-old intact female beagle dog (I–K), respectively. Venular components of the CAHO pathways are readily visualized following both angiographic techniques and are depicted by the *arrows*. Visualization of terminal ciliary arterioles and conjunctival vasculature (*arrowhead*) is noted following IV angiography alone. For comparative purposes, representative digital overlays and color renderings of angiographic images were generated following IC AA and IV SA utilizing ICG (D, H, L). Digital overlay and color rendering of images were performed utilizing an imaging editing software. Color rendering was performed using the color range tool (entire image), isolating observed fluorescence patterns. *Red* indicates fluorescence observed following IC AA, and *blue* indicates fluorescence observed following IV SA. Note partial luminal filling of the larger vascular channels following IC AA (*black arrows*), suggestive of laminar flow. Image acquisition times following ICG injection included the following; B (5 minutes), C (5 minutes), F (8 minutes), G (1 minute), J (1 minute), and K (2 minutes).

procedure all eyes were noted to exhibit 1+ aqueous flare, which resolved with medical therapy 2 days post-procedure. Two dogs were observed to have developed a small amount of fibrin and mild generalized flare (4+ grading on the SUN scale) that subsequently resolved over the course of 10 days. Following IV SA, no adverse systemic or ocular signs were observed.

## Discussion

To the authors' knowledge, this is the first study documenting distal aqueous humor outflow in live dogs with no known ocular abnormalities. The results of this study demonstrated that AA, using similar delivery techniques as in humans,<sup>15,20,22</sup> was easy to



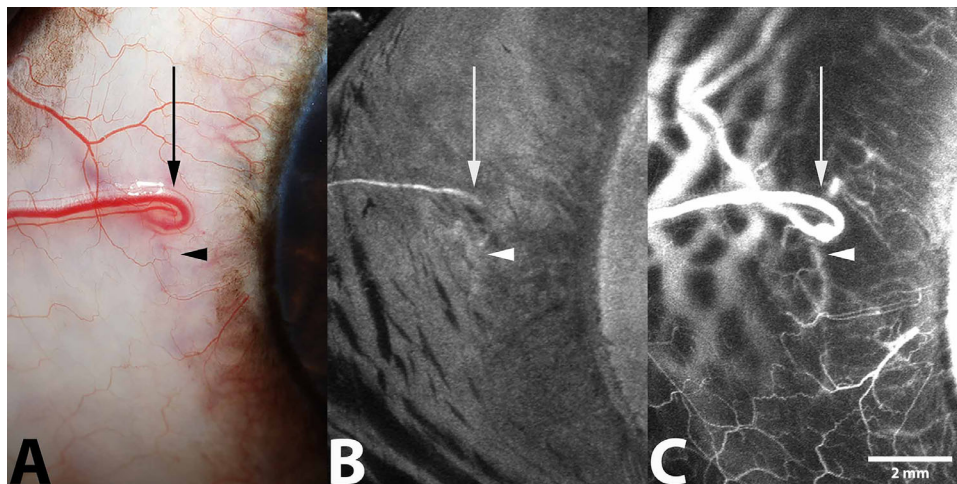


**Figure 9.** Representative (A) standard color, (B) IC AA (17 minutes after ICG injection), and (C) IV SA (5 minutes after ICG injection) from the right eye of a 4-year-old male mixed-breed dog. This eye demonstrated minimal visualization of the CAHO pathways following IC administration of ICG. Outflow occurred via a component of the intrascleral plexus (*arrowhead*) and an episcleral vein (*arrow*). These components are similarly visible using standard color and IV ICG angiography.

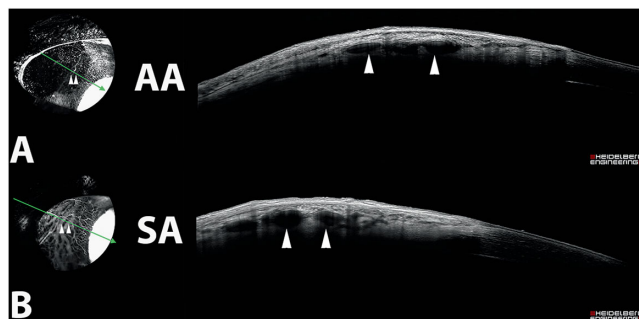


**Figure 10.** Cross-sectional OCT scans from the right eye of a 3-year-old intact female beagle dog following IC (A) and IV (B) ICG angiography. The orientation of the scan (*green arrow*) depicts luminal vessels that demonstrated fluorescence following both angiographic modalities (*arrowhead*) in similar locations within the tissue.

perform in cadaver eyes of dogs and permitted visualization of the CAHO pathways. This is consistent with recent studies in ex vivo canine and feline models<sup>23,24,35</sup> (McLellan GJ, et al. *IOVS*. 2019;60:ARVO Abstract 3184). Unfortunately, utilizing the same approach and delivery system, the authors were unable to attain comparable results in live dogs. Modification of the IC delivery to a more clinically applicable single-bolus injection technique permitted visualization of the angiographic dye within the CAHO pathways.

Similarities were observed in the location, size, pattern, and redundancy of vascular components associated with CAHO pathways between IC and IV dye administration, consistent with those of previous corrosion casting techniques.<sup>2,36</sup> Cross-sectional

OCT images supported the notion that vessels observed were the deep intrascleral plexus and venous circle of Hovius.<sup>1,2</sup> Although the use of sodium fluorescein and ICG permitted clear visualization of the CAHO pathways ex vivo, rapid diffusion of sodium fluorescein, presumably due to its small molecular size and binding properties,<sup>33,37–39</sup> occurred. As such, ICG was employed for subsequent in vivo AA.

Use of the gravity-fed trocar system was shown to be effective for administering ICG into the anterior chamber of the living dog eye; however, no subsequent flow of dye within the CAHO pathways or its vascular components could be visualized. This finding may have simply reflected the dynamic nature of aqueous humor outflow and the variation in CAHO pathways. As demonstrated in humans, visualization of the CAHO pathway is often intermittent, not continuous.<sup>5</sup> It is possible that sectors exhibiting outflow did not coincide with the area being observed. Inter-individual differences in vascular patterns and scleral or conjunctival pigmentation, as well as species differences in sectoral outflow of aqueous humor, may also have hindered visualization of the angiographic signal.<sup>40,41</sup> Although the above are all possible explanations, the authors believe the lack of observation of dye fluorescence most likely reflected the experimental setup itself and its inability to be directly transferred for use in dogs due to anatomical differences. Placement of the trocars was limited to the temporal half of the globe due to the natural degree of scleral exposure; although permitting safe insertion into the globe, the collar of the trocars often interfered with the eyelid speculum and/or with



the eyelids themselves. As a result, compressive effects on the sclera may have occurred due to the trocar collars alone or in conjunction with the eyelid and/or eyelid speculum, leading to a lack of detectable fluorescence within the CAHO pathways.

Modification to an *in vivo* single bolus IC injection resulted in clear visualization of dye within CAHO pathways. The volume of ICG dye administered was comparable between dogs of similar body weights, and the rate of dye administration was approximately the same when introduced under steady pressure as a bolus injection. This bolus approach was significantly less time consuming, relied on a simplified experimental setup, and resulted in subjectively lower scores of post-procedure intraocular inflammation as compared to the gravity-fed delivery system. Although human eyes are more tolerant and generate less of an inflammatory response to such procedures,<sup>15</sup> dog eyes are known to exhibit a significantly greater inflammatory response, even following minimally invasive intraocular procedures.<sup>42</sup> As such, the IC approach may be more advantageous in clinical veterinary practice, permitting AA to be more readily performed with less intraocular irritation or trauma. Additionally, the use of heavy sedation in lieu of general anesthesia was effective for patient positioning, rotation of the globe, and conducting AA. Sedation facilitated a faster recovery of the dogs and reduced associated costs, thereby enhancing the feasibility of AA as a potential clinical diagnostic tool.

In contrast to human studies,<sup>15</sup> due to the presence of a nictitating membrane nasally, a deeper orbit, and a larger corneal diameter, scleral exposure of the dog eyes was limited and prohibited visualization of the inferior, nasal, and superonasal scleral sectors<sup>24</sup> (McLellan GJ, et al. *IOVS*. 2019;60:ARVO Abstract 3184). Based on eyelid conformation, the temporal scleral sector was the easiest to image in dogs, followed by the superotemporal and inferotemporal sectors. The superior and inferior scleral sectors were the most challenging to clearly visualize. In lieu of an eyelid speculum, two conjunctival stay sutures were utilized to help manipulate the globe while relying on manual retraction of the eyelids, with careful attention not to apply pressure to the globe or to the eyelids.<sup>5</sup> Although there are limitations to this method of scleral exposure, including possible distortion or compression of aqueous humor outflow pathways, the authors had no other option than to open the eyelids in sedated and/or anesthetized dogs.

As the superonasal sector was injected, we anticipated strong dye fluorescence in the inferotemporal sector due to its location directly opposite the injection site; however, this was not the case. Sectoral variation in

dye fluorescence was noted, with the most common site of dye visualization being in the superotemporal sector of the sclera. Two dogs, 1.6 and 2.2 years old, demonstrated no fluorescence of dye after IC administration of ICG. At this time, we can only speculate on reasons for the lack of dye visibility in two of the 12 eyes (16.7%), such as low levels of aqueous outflow, sectoral outflow, or dilution of dye within the anterior chamber. Fluctuations in IOP could cause sudden collapse of the outflow pathways and/or possible dye leakage following IC injection, resulting in varied concentrations of dye within the anterior chamber. Approximately 98% of ICG dye in plasma appears protein bound,<sup>43</sup> consistent with our observation of steady fluorescence within the scleral vasculature after an initial flux in the intensity of ICG dye and minor leakage into the surrounding tissues. Despite there being no apparent differences in the permeability of ICG dye associated with age, it is possible that the age of the dogs could also have played a role. Two cadaver eyes originated from a 2-month old puppy, but all of the live dogs evaluated in this study were adults under the age of 5.9 years. It is unknown at this time if older dogs have an observable difference in sectoral outflow of ICG dye compared to juvenile dogs. Given this information, the authors are working toward a quantitative method to measure intensity signals of fluorescent dye to allow for objective evaluation and comparison of dye outflow.

Although they were not a primary focus of this study, two interesting observations noted during the current study included pulsatile dye movement within the CAHO pathways during AA and varied fluorescent patterns following direct comparisons between IC and IV routes of dye administration. Of the 10 eyes that demonstrated progressive fluorescence after IC administration of ICG, four eyes exhibited visible pulsation and turbulent movement of ICG, and two eyes demonstrated visible bidirectional flow of dye. These observations have been similarly described in human subjects,<sup>15,20</sup> highlighting the dynamic nature of these outflow pathways. The pulsatile dye movement, given its rhythmic nature with the heart rate of the dog, was believed to reflect transient and minute IOP fluctuations generated by alterations in blood pressure during systole.<sup>29</sup> In humans, this pulsatile movement has been demonstrated *in vivo* and is suspected to be linked to a cyclic flow pattern of aqueous initially induced by elevations in IOP from blinking and eye movement<sup>44</sup> followed by a piston-like action of the choroid as a result of cardiac pulsation.<sup>45</sup> The result of this cyclic flow is a surge of aqueous humor into systemic circulation during the peak radial pulse.<sup>27</sup> Although our study evaluated normal dogs, we speculate that the degree

and frequency of this pulsatile dye movement may be reduced or eliminated during elevations in IOP.

In the current study only a small volume of dye was administered IC. Although IOP was unable to be measured immediately after injection due to limitations in the time frame necessary to obtain angiogram images, IOP was measured 15 minutes following completion of angiography. Intraocular pressure exceeded the upper limits of the normal reference range (22 mm Hg) in only one eye (25 mm Hg),<sup>31</sup> which returned to normal (below 22 mm Hg) within 1 hour. Although alterations in dye concentration within the aqueous humor may have occurred using a single-bolus approach, variations were considered minimal and were not believed to have affected the study results. Scleral imaging following IV administration of ICG readily identified the venous components associated with the CAHO pathways, similar to IC administration, including the intrascleral plexus and the venous circle of Hovius. Results herein were consistent with corrosion casts, which identified ciliary vessels running circumferentially through the sclera, immediately anterior to the scleral venous plexus; these vessels branched into anterior ciliary arteries, then split into various arteriolar branches before forming a capillary bed at the limbus.<sup>2</sup>

Direct comparison between IC and IV dye administration demonstrated stratification of dye, specifically following IC administration as dye entered into the systemic circulation at the level of the circle of Hovius. In contrast, IV administration resulted in progressive and uniform luminal filling of the observed vasculature. This suggested that laminar aqueous humor outflow was occurring with IC administration of dye, a finding similarly noted in human and porcine eyes.<sup>28,30,44,46</sup> This was thought to reflect the movement and bipartite separation of aqueous humor from the sanguineous components of blood (blood corpuscles) as it entered into hematogenous circulation.<sup>27</sup> This observation was inconsistent, and its absence may have simply reflected anatomical variations between subjects resulting from two distinct but intimately associated intervening small vessels, separated by a minute physical distance. Alternatively, the absence of laminar flow may have occurred due to the formation of a smooth and continuous solitary column of aqueous humor within a single larger vessel, resulting in a tripartite stratification pattern and the appearance of two vascular channels.<sup>30</sup>

An additional challenge of AA is the standardization of numerous parameters. Identical scleral sectors between subjects need to be imaged, utilizing identical dye volume, dye concentration, rate of infusion, illumination, and filter settings. Additionally, IOP is

an important variable that must be considered when evaluating aqueous humor outflow. Normal morphology, structural composition, and the array of dynamic physiologic changes that can arise in different ages and/or breeds of dogs should also be considered.<sup>47</sup> The heterogeneous results recorded herein before and after AA and SA imaging indicated poor control of IOP between eyes and is a limitation of this study. Alterations in IOP may be an effect of the drugs employed for conducting angiography or the technique itself. Numerous sedative and anesthetic drug protocols have demonstrated alterations in IOP and aqueous outflow.<sup>4,48</sup> Intracameral administration may have induced a rise in IOP accounting for transient elevations following bolus dye administration. Alternatively, minute leakage via the needle tract and/or induction of mild anterior uveitis following IC injection may have accounted for the lower IOPs noted in some cases. It has been speculated that the rapid influx of fluid into the anterior chamber results in incomplete mechanical disruption of the aqueous outflow barriers, including the blood–aqueous barrier<sup>36</sup>; however, the significance of these IOP alterations and their true impact on aqueous humor outflow facility remain unknown. Controversy exists within the literature regarding canine IOPs and their correlation with aqueous humor outflow. Tonography and fluorophotometry studies have demonstrated elevations in IOP yield increased rates of aqueous humor outflow.<sup>4,48</sup> Conversely, using a perfusion model, outflow facility has been reported to be relatively stable and independent of IOP alterations.<sup>36</sup>

The washout effect may contribute to changes in aqueous humor outflow. This phenomenon has been well described in many species<sup>49</sup> to take effect as early as 30 minutes after perfusing the globe.<sup>50,51</sup> In canines, washout is suspected to be primarily due to disruption and/or removal of the hyaluronidase-sensitive component of the barriers to aqueous outflow and not a direct IOP effect.<sup>11,36</sup> As such, it is possible that perfusion for 1 hour prior to angiography may have impacted aqueous outflow in ex vivo eyes. To limit the impact on eyes evaluated in this study, all eyes were treated similarly. It is also reasonable to conclude that transient IOP alterations likely impact aqueous outflow facility to some degree in the eyes of live dogs.<sup>36</sup> This, coupled with highly variable IOP values in this study, could be a potential confounder of aqueous outflow which could have altered the angiographic signal visualized and the timing observed. Future studies are required to address these limitations, wherein IOP is less varied in order to determine if IOP and washout have a true impact on aqueous humor outflow.

## Conclusions

Descriptive findings of CAHO pathways *ex vivo* and *in vivo* in normal dogs were provided. Scleral angiography with ICG appears to be an effective means for identifying the vascular components associated with the distal CAHO pathways, whereas AA permits visualization and qualitative assessment of aqueous humor outflow. This study demonstrated the capacity to visualize distal CAHO pathways following AA in dogs using the proposed IC experimental set up and imaging device. The information provided herein offers new insights into the fluid characteristics associated with the CAHO pathways of dogs, which could serve as the foundation for subsequent studies. This imaging modality could have an immediate benefit in dogs by identifying a clinically applicable tool to evaluate the CAHO pathways *in vivo*. This could shed new insights into the characteristics of CAHO pathways and how they may become altered in a variety of sight-threatening conditions. Ultimately, it may allow for patient-specific therapeutic approaches aimed at controlling IOP and preserving vision.

## Acknowledgments

The authors thank the animal care team at the vivarium of the Michigan State University College of Veterinary Medicine for their assistance in caring for the dogs. The authors also thank Gillian J. McLellan, PhD, and her laboratory team at the University of Wisconsin–Madison for their input regarding AA techniques. The authors also recognize Laurence Occelli, PhD, for her technical assistance with imaging and data management.

Supported by Michigan State University College of Veterinary Medicine Endowed Research Funds; Michigan State University startup funds; grants from the National Institutes of Health (R01-EY025752, NIH K08EY024674); the Bright Focus Foundation; Research to Prevent Blindness Career Development Award; and Research to Prevent Blindness unrestricted grant to UCLA.

Disclosure: **J.B. Burn**, None; **A.S. Huang**, None; **A.J. Weber**, None; **A.M. Komáromy**, None; **C.G. Pirie**, None

## References

1. van Buskirk EM. The canine eye: the vessels of aqueous drainage. *Invest Ophthalmol Vis Sci.* 1979;18:223–230.
2. Sharpnack DD, Wyman M, Anderson BG, Anderson WD. Vascular pathways of the anterior segment of the canine eye. *Am J Vet Res.* 1984;45:1287–1294.
3. McMaster PRB, Macri FJ. Secondary aqueous humor outflow pathways in the rabbit, cat, and monkey. *Arch Ophthalmol.* 1968;79:297–303.
4. Peiffer RL, Gelatt KN, Gum GG. Determination of the facility of aqueous humor outflow in the dog, comparing *in vivo* and *in vitro* tonographic and constant pressure perfusion techniques. *Am J Vet Res.* 1976;37:1473–1477.
5. Huang AS, Li M, Yang D, Wang H, Wang N, Weinreb RN. Aqueous angiography in living non-human primates shows segmental, pulsatile, and dynamic angiographic aqueous humor outflow. *Ophthalmology.* 2017;124:793–803.
6. Gelatt KN, Gum GG, Williams LW, Barrie KP. Uveoscleral flow of aqueous humor in the normal dog. *Am J Vet Res.* 1979;40:845–848.
7. Johnson M, McLaren JW, Overby DR. Unconventional aqueous humor outflow: A review. *Exp Eye Res.* 2017;158:94–111.
8. Bedford PGC, Grierson I. Aqueous drainage in the dog. *Res Vet Sci.* 1986;41:172–186.
9. Samuelson DA, Gum GG, Gelatt KN. Ultrastructural changes in the aqueous outflow apparatus of beagles with inherited glaucoma. *Invest Ophthalmol Vis Sci.* 1989;30:550–561.
10. Barrie KP, Gum GG, Samuelson DA. Quantitation of uveoscleral outflow in normotensive and glaucomatous Beagles by 3H-labeled dextran. *Am J Vet Res.* 1985;46:84–88.
11. van Buskirk EM, Brett J. The canine eye: *in vitro* studies of the intraocular pressure and facility of aqueous outflow. *Assoc Res Vis Ophthalmol.* 1973;17:373–377.
12. Alm A, Nilsson SFE. Uveoscleral outflow: a review. *Exp Eye Res.* 2009;88:760–768.
13. Waxman S, Wang C, Dang Y, et al. Structure–function changes of the porcine distal outflow tract in response to nitric oxide. *Invest Ophthalmol Vis Sci.* 2018;59:4886–4895.
14. Andrew NH, Akkach S, Casson RJ. A review of aqueous outflow resistance and its relevance to microinvasive glaucoma surgery. *Surv Ophthalmol.* 2020;65:18–31.

15. Huang AS, Camp A, Xu BY, Penteadó RC, Weinreb RN. Aqueous angiography: aqueous humor outflow imaging in live human subjects. *Ophthalmology*. 2017;124:1249–1251.
16. Akagi T, Uji A, Huang AS, et al. Conjunctival and intrascleral vasculatures assessed using anterior segment optical coherence tomography angiography in normal eyes. *Am J Ophthalmol*. 2018;196:1–9.
17. Alario AF, Pirie CG. Fluorescein gonioangiography of the normal canine eye using a dSLR camera adaptor. *Res Vet Sci*. 2015;100:277–282.
18. Pirie CG, Alario A. Anterior segment angiography of the normal canine eye: a comparison between indocyanine green and sodium fluorescein. *Vet J*. 2014;199:360–364.
19. Zhou XX, Liu AH, Lin S, Wu JG. A simultaneous iris angiography technique in pigmented rabbits. *Ophthalmic Res*. 2012;47:109–112.
20. Huang AS, Saraswathy S, Dastiridou A, et al. Aqueous angiography with fluorescein and indocyanine green in bovine eyes. *Transl Vis Sci Technol*. 2016;5:5.
21. Huang AS, Saraswathy S, Dastiridou A, et al. Aqueous angiography-mediated guidance of trabecular bypass improves angiographic outflow in human enucleated eyes. *Invest Ophthalmol Vis Sci*. 2016;57:4558–4565.
22. Saraswathy S, Tan JCH, Yu F, et al. Aqueous angiography: real-time and physiologic aqueous humor outflow imaging. *PLoS One*. 2016;11:e0147176.
23. Snyder KC, Oikawa K, Williams J, et al. Imaging distal aqueous outflow pathways in a spontaneous model of congenital glaucoma. *Transl Vis Sci Technol*. 2019;8:22.
24. Telle MR, Snyder KC, Teixeira LBC, et al. Development and validation of new methods to visualize conventional aqueous outflow pathways in canine glaucoma. *Vet Ophthalmol*. 2019;22:E32.
25. McLellan GJ, Snyder KC, Oikawa K, Kiland JA, Gehrke S, Huang AS. Imaging distal aqueous outflow pathways in a spontaneous model of primary congenital glaucoma (PCG). *Invest Ophthalmol Vis Sci*. 2018;59:5908.
26. Roy S, Boldea R, Perez D, Curchod M, Mermoud A. Visualisation du système d'écoulement de l'humeur aqueuse chez le lapin avec la fluoresceine et le vert d'indocyanine. *Klin Monbl Augenheilkd*. 2000;216:305–308.
27. Ascher K. The aqueous veins: I. Physiologic importance of the visible elimination of intraocular fluid. *Am J Ophthalmol*. 1942;25:1174–1209.
28. Francis AW, Kagemann L, Wollstein G, et al. Morphometric analysis of aqueous humor outflow structures with spectral-domain optical coherence tomography. *Invest Ophthalmol Vis Sci*. 2012;53:5198–5207.
29. Li P, Shen TT, Johnstone M, Wang RK. Pulsatile motion of the trabecular meshwork in healthy human subjects quantified by phase-sensitive optical coherence tomography. *Biomed Opt Express*. 2013;4:2051–2065.
30. Johnstone M, Martin E, Jamil A. Pulsatile flow into the aqueous veins: manifestations in normal and glaucomatous eyes. *Exp Eye Res*. 2011;92:318–327.
31. Tofflemire KL, Wang C, Jens JK, Ellinwood NM, Whitley RD, Ben-shlomo G. Evaluation of three hand-held tonometers in normal canine eyes. *Vet J*. 2017;224:7–10.
32. Camras LJ, Stamer WD, Epstein D, Gonzalez P, Yuan F. Differential effects of trabecular meshwork stiffness on outflow facility in normal human and porcine eyes. *Invest Ophthalmol Vis Sci*. 2012;53:5242–5250.
33. Gelatt KN, Henderson JD, Steffen GR. Fluorescein angiography of the normal and diseased ocular fundi of the laboratory dog. *J Am Vet Med Assoc*. 1976;169:980–984.
34. Jabs DA, Nussenblatt RB, Rosenbaum JT, Standardization of Uveitis Nomenclature (SUN) Working Group. Standardization of uveitis nomenclature for reporting clinical data. Results of the First International Workshop. *Am J Ophthalmol*. 2005;140:509–516.
35. Snyder K, Oikawa KSG, Gehrke S, et al. Dynamic imaging of distal aqueous humor outflow pathways in feline congenital glaucoma (FCG). *Vet Ophthalmol*. 2019;22:E31.
36. van Buskirk E, Brett J. The canine eye: in vitro dissolution of the barriers to aqueous outflow. *Invest Ophthalmol Vis Sci*. 1978;17:258–263.
37. Flower RW, Hochheimer BF. A clinical technique and apparatus for simultaneous angiography of the separate retinal and choroidal circulation. *Invest Ophthalmol Vis Sci*. 1973;12:248–261.
38. Wakaiki S, Maehara S, Abe R, et al. Indocyanine green angiography for examining the normal ocular fundus in dogs. *J Vet Med Sci*. 2007;69:465–470.
39. Yuzawa M, Kawamura A, Matsui M. Clinical evaluation of indocyanine green video angiography in the diagnosis of choroidal neovascular membrane associated with age-related macular degeneration. *Eur J Ophthalmol*. 1992;1:115–121.



40. Waxman S, Loewen RT, Dang Y, Watkins SC, Watson AM, Loewen NA. High-resolution, three-dimensional reconstruction of the outflow tract demonstrates segmental differences in cleared eyes. *Invest Ophthalmol Vis Sci.* 2018;59:2371–2380.
41. Wecker T, van Oterendorp C, Reichardt W. Functional assessment of the aqueous humour distal outflow pathways in bovine eyes using time-of-flight magnetic resonance tomography. *Exp Eye Res.* 2018;166:168–173.
42. Azoulay T, Dulaurent T, Isard P, Poulain N, Goulle F. Chirurgie de la cataracte bilatérale immédiatement séquentielle chez le chien: une étude rétrospective de 128 cas (256 yeux). *J Fr Ophthalmol.* 2013;26:645–651.
43. Maarek JI, Holschneider DP, Harimoto J. Fluorescence of indocyanine green in blood: intensity dependence on concentration and stabilization with sodium polyaspartate. *J Photochem Photobiol B Biol.* 2001;65:157–164.
44. Ascher K. *The Aqueous Veins, Vol. 1.* Springfield, IL: Charles C Thomas; 1961.
45. Phillips C, Tsukahara S, Hosaka O, Adams W. Ocular pulsation correlates with ocular tension: the choroid as piston for an aqueous pump? *Ophthalmic Res.* 1992;24:338–343.
46. Wang B, Kagemann L, Schuman JS, et al. Gold nanorods as a contrast agent for Doppler optical coherence tomography. *PLoS One.* 2014;9:e90690.
47. Gelatt K, Gwin R, Peiffer R Jr, Gum G. Tonography in the normal and glaucomatous beagle. *Am J Vet Res.* 1977;38:515–520.
48. Ward DA, Cawrse MA, Hendrix DVH. Fluorophotometric determination of aqueous humor flow rate in clinically normal dogs. *Am J Vet Res.* 2001;62:853–858.
49. Gong H, Freddo TF. The washout phenomenon in aqueous outflow - why does it matter? *Exp Eye Res.* 2009;88:729–737.
50. Kaufman P, True-Gabelt B, Erickson-Lamy K. Time-dependence of perfusion outflow facility in the cynomolgus monkey. *Curr Eye Res.* 1988;7:721–726.
51. Erickson K, Kaufman P. Comparative effects of three ocular perfusates on outflow facility in the cynomolgus monkey. *Curr Eye Res.* 1981;1:211–216.

## Supplementary Material

**Supplementary Movie S1.** Video footage obtained from the right eye of 3-year-old intact female beagle dog following IC injection of ICG for conducting AA. Note the dynamic and pulsatile nature of dye movement within the CAHO pathways following IC injection.

**Supplementary Movie S2.** Video footage obtained from the right eye of 3-year-old intact female beagle (same eye from Supplementary Movie S1) following IV administration of ICG for conducting SA. Turbulent dye movement was noted only during the initial filling phase following IV administration of ICG.